

Research Paper

Cite this article: Azari-Nasab T, Ghobadi CH, Azarm B, Majidzadeh M (2020). Triple-band operation achievement via multi-input multi-output antenna for wireless communication system applications. *International Journal of Microwave and Wireless Technologies* **12**, 259–266. <https://doi.org/10.1017/S1759078719001302>

Received: 15 December 2018

Revised: 8 September 2019

Accepted: 13 September 2019

First published online: 10 October 2019

Keywords:

MIMO antenna; triple band performance; WiMAX; WLAN

Author for correspondence:

B. Azarm, E-mail: st_b.azarm@urmia.ac.ir

Triple-band operation achievement via multi-input multi-output antenna for wireless communication system applications

T. Azari-Nasab¹, CH. Ghobadi², B. Azarm²  and M. Majidzadeh³

¹Electrical Engineering Department, Aeen Kamal University, Urmia, Iran; ²Electrical Engineering Department, Urmia University, Urmia, Iran and ³Department of Electrical and Computer Engineering, Urmia Girls Faculty, West Azarbaijan Branch, Technical and Vocational University, Urmia, Iran

Abstract

A multi-input multi-output (MIMO) antenna is designed and discussed for multi-band applications. The constituent antennas are composed of four L-shaped elements and a ground plane. When placed beside each other to form a MIMO antenna, a T-bar shaped parasitic structure is also embedded between the antennas on the backside of the substrate to increase the inter-element isolation. The triple-band performance of the antenna is observed at 2.15–2.73 GHz, 3.1–3.9 GHz, and 5.04–6 GHz. The isolation level of more than 20 is seen over the operating frequency range. The fabricated prototype of the MIMO antenna size is very compact (20 × 40 mm), printed on the FR4 substrate. Based on simulation and experimental results, the proposed design is useful for WiMAX and WLAN applications.

Introduction

Recently multi-input multi-output (MIMO) antennas have gained popularity owing to their suitable performance in different communication applications. Multi band notched applications [1–3], Hyperlan, WiMAX, and WLAN applications [4–6], ISM band applications [7], WiFi and LTE applications [8–10], GPS/UMTS [11], GSM, PCS, LTE2300, and 5 G bands [12] are some of the possible applications for these antennas. “MIMO” antenna term is dedicated to a technology in which more than one antenna are adopted on both source and destination sides. The adjacency of many antennas in a MIMO system, although yield marvelous outputs, but simultaneously brings about some challenges. The most important of them is the coupling problem. When the antennas work close to each other, the coupling effect between them influences the performance of the others. This in turn deteriorates the antenna overall radiation characteristics. Hence, a suitable solution should be provided to get the most out of MIMO antennas. There has been a vast variety of research studies dedicated for isolation improvement. For instance in [13] a compact MIMO antenna is proposed for 2.4 GHz WLAN applications. The high inter-element isolation is obtained by suitable adoption of a defected shorting wall. In this way, better than –20 dB isolation is achieved with a maximum of –43 dB at the central frequency. As another example, the authors in [14] have surveyed a compact broadband MIMO antenna in which the isolation is obtained by locating the constituent antennas orthogonal to each other. This minimizes the coupling and yields a better performance. In [15] by adding parasitic elements in the MIMO antenna structure, a double-coupling path is introduced which creates a reverse coupling and yields mutual coupling reduction. Although interesting results have been proposed in the literature, but the challenges the MIMO antennas face, still require more attention and discussion. Proposing novel decoupling methods, size miniaturization, and design of novel antenna structures are the topics in this area.

Moreover, it should be kept in mind that in MIMO systems, due to the contribution of many single antennas, almost a bulky volume is needed for the antenna to be installed. Hence, the compactness of the both single and MIMO antennas is an important factor which should be considered in a design process.

In this paper, a two-element MIMO antenna is proposed. The proposed antenna topology is composed of two antennas each of them consists of a simple ground plane on the backside and a combination of L-shaped elements with different lengths on top side. Proper embedment of the conductive elements yields a triple-band operation for the single antenna with focus at WiMAX and WLAN frequency bands. Similarly, the proposed two-element MIMO antenna structure exhibits a triple band operation. Moreover, the adopted simple parasitic element enhances the inter-element isolation significantly. The obtained merits through the proposed structure are summarized as follows:

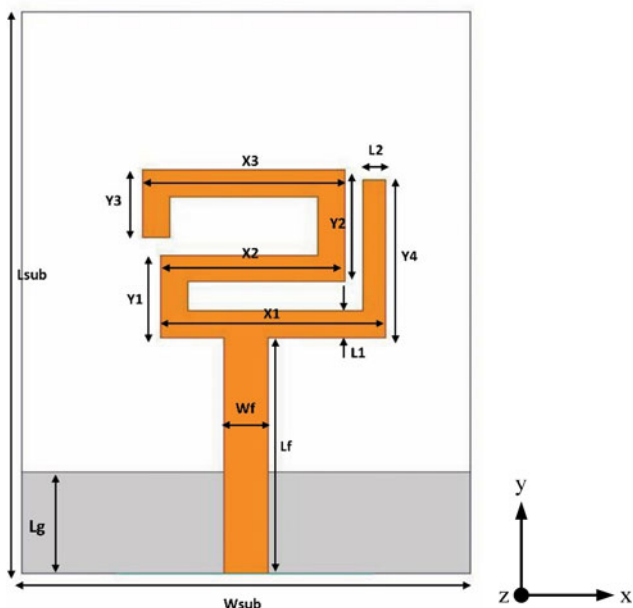


Fig. 1. The proposed single antenna configuration and parameters.

Table 1. Comparison of proposed MIMO antennas with some of antennas recently reported in papers

Ref	Element number	Size (mm ²)	Operating bands (GHz)	Isolation
[18]	4	100 × 60	1.975–2.080, 2.160–2.230, 2.350–2.620, 3.060–3.140, 3.480–3.540, 16.50–17.80	–10
[19]	2	50 × 50	2.09–2.86, 5.05–5.94	–17.8
[20]	2	36 × 40	2.4–2.484, 3.4–3.69, 5.15–5.825	–15
[21]	2	60 × 15	0.740–0.965, 1.380–2.703	–10
[22]	2	17 × 42	6.6–7.6, 8.3–10	–13
[23]	2	21 × 90	2.22–2.54, 3.14–3.9, 5.3–5.7	–20
This work	2	20 × 40	2.15–2.73, 3.1–3.9, 5.04–6	–20

- Proposing a simple-structured and cost effective single antenna.
- Achieving a triple-band operation through the proposed compact single antenna with focus at in-service frequency bands of WiMAX and WLAN.
- Designing a two-element MIMO antenna with compact dimensions with respect to most of the previously designed two-element MIMO antennas.
- Obtaining a high-isolation level in the MIMO antenna through a simple decoupling element.

This paper is organized in different sections as explained below: In section “Single antenna design and performance”, a single antenna element is proposed and discussed as the constituent

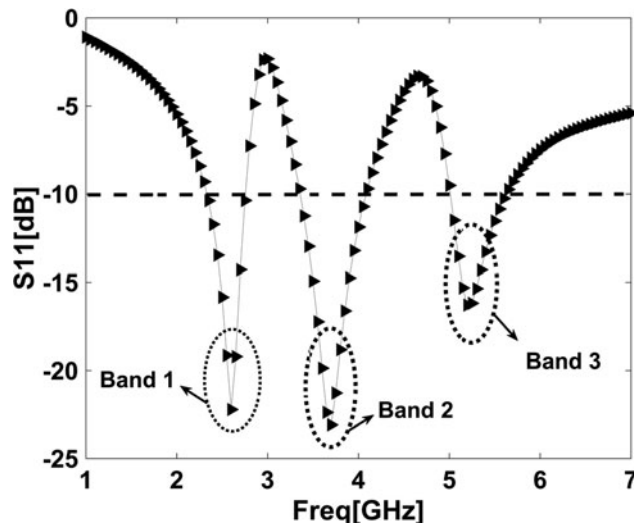


Fig. 2. Simulated S₁₁ curve for the proposed single antenna.

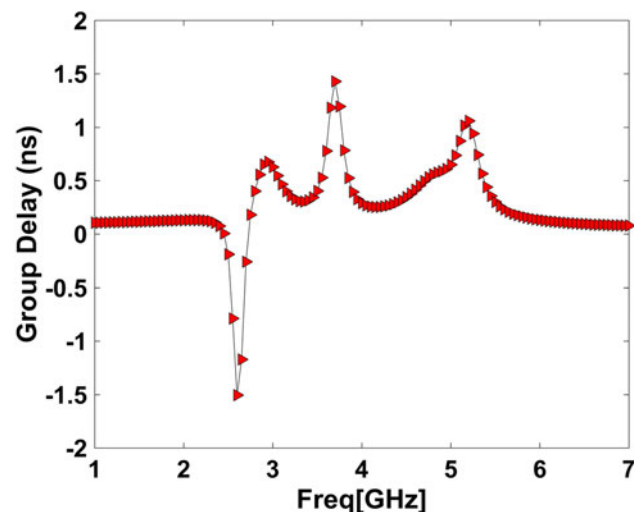


Fig. 3. Simulated group delay for the proposed single antenna.

element of the MIMO antenna. Then, section “MIMO antenna configuration” introduces the proposed MIMO antenna configuration with two of the aforementioned monopole antennas. In the sequel, in section “MIMO antenna performance analysis”, MIMO antenna performance is discussed in detail. The effect of the embedded slots, the isolating parasitic element, and MIMO antenna performance based on surface current distribution are released in this section. Measured results and their comparison with simulated ones are presented in section “Results and discussion”. Then, with the aim of highlighting the advantages of the proposed MIMO antenna over the similar previous designs, a comparison is established in section “Comparison”. Ultimately section “Conclusion” concludes the paper.

Single antenna design and performance

The proposed single antenna design is shown in Fig. 1. As can be seen, the radiating patch is composed of the combinations of L-shaped elements which are suitably connected to each other.

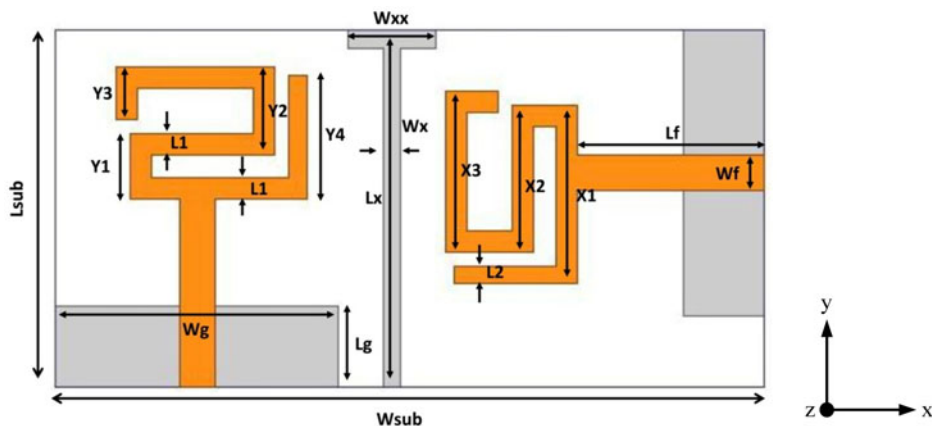


Fig. 4. Configuration of the proposed two-element MIMO antenna.

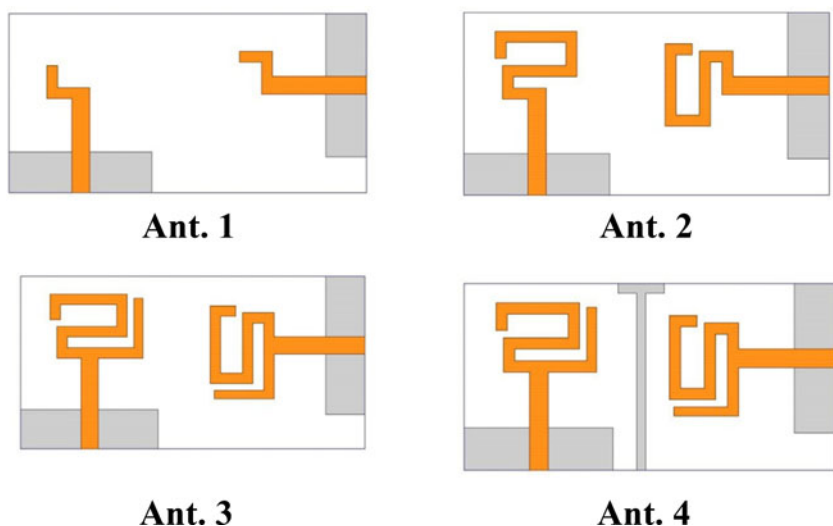


Fig. 5. The MIMO antenna design process.

As can be seen the overall size of the antenna is $20 \times 20 \text{ mm}^2$. A simple rectangular microstrip feed line with length and width of $L_f = 10.5 \text{ mm}$ and $W_f = 2 \text{ mm}$ excites the antenna structure. Moreover, a rectangular ground plane is placed on the backside of the substrate. The antenna with the given values in Table 1 is simulated using finite element method-based high-frequency structure simulator [16] software and the relevant S_{11} curve is plotted in Fig. 2. Based on the results in this figure, a triple-band operation with central frequencies of 2.6, 3.7, and 5.2 GHz is obtained for the proposed single antenna. The obtained frequency ranges are in line with WiMAX and WLAN frequency bands. It should be noted that each conductive element plays an important role in the formation of the antenna final performance. Herein, it is seen that three resonances are excited in the S_{11} curve. This observation means that there are some elements which influence the surface current distribution at special resonances, yielding a resonance in the antenna S_{11} curve. Herein, each resonance is excited by one of the branches in the radiating patch. The governing formula which clarifies the relationship between the excited resonances and antenna structural and physical features is as follows [17]:

$$f = \frac{c}{2L_e \sqrt{\epsilon_{re}}} \quad (1)$$

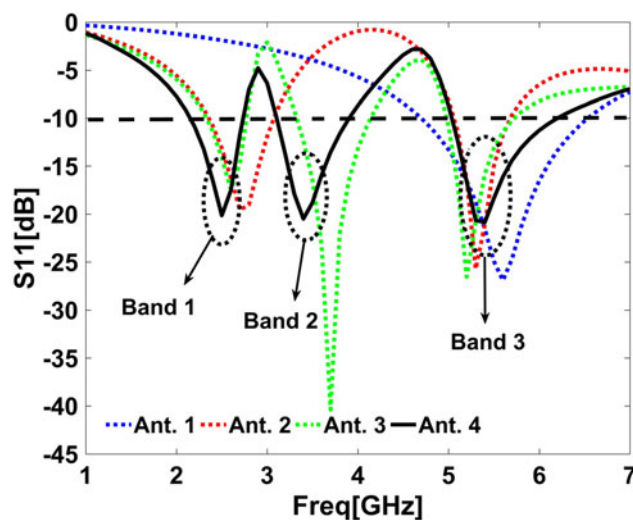


Fig. 6. S_{11} curves for different antennas in the MIMO design process in Fig. 5.

where L_e is the electric length of the included conductive elements, and ϵ_{re} relates to the antenna substrate material. It is clear that suitable placement of conductive elements and proper

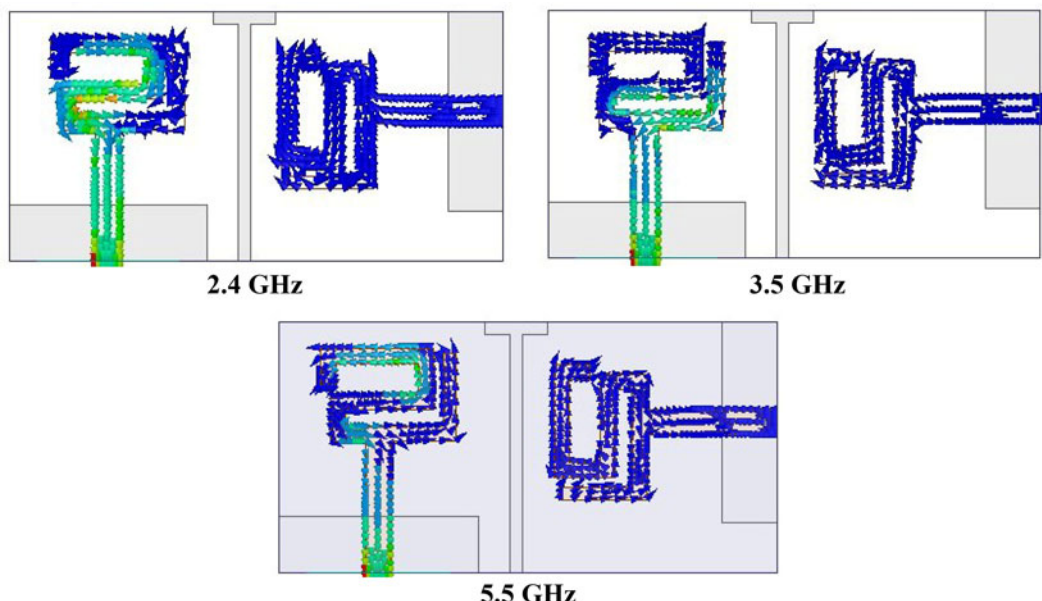


Fig. 7. Surface current distribution on the proposed MIMO antenna.

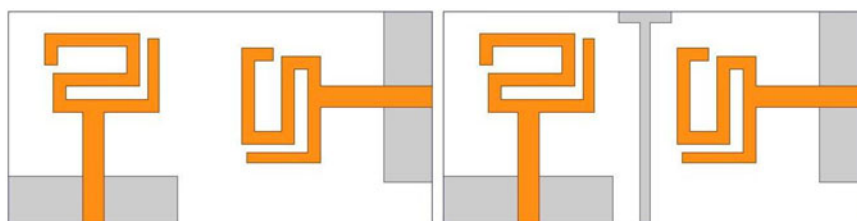


Fig. 8. MIMO antenna with and without T-bar parasitic element.

tuning of their dimensions would yield a desired performance focused on applicable frequency bands.

Moreover, to investigate the time-domain characteristics of the proposed antenna, the group delay curve is also plotted in Fig. 3. Based on the obtained results, the group delay variation is less than 2 ns which is considered a suitable range for different applications in communication systems.

MIMO antenna configuration

The proposed MIMO antenna is shown in Fig. 4. As mentioned before, the constituent elements are simple monopole antennas discussed in previous section. The total size of the proposed two-element MIMO antenna is $20 \times 40 \text{ mm}^2$ which is considered a compact structure with easy installation in communication systems and applications. As a well-known fact, when the antennas perform in a close distance from each other, they affect each other. One method to reduce this undesired effect is the embedment of parasitic structures between the antennas. With the aim of isolation enhancement, a T-bar element is included between the monopole antennas on the backside of the substrate. Detailed values of the proposed design are as follows: All the values are in millimeters. $W_{sub} = 40 \text{ mm}$, $L_{sub} = 20 \text{ mm}$, $L_g = 4.5 \text{ mm}$, $L_f = 10.5 \text{ mm}$, $W_f = 2 \text{ mm}$, $W_g = 16 \text{ mm}$, $W_x = 1 \text{ mm}$, $L_x = L_{sub}$, $W_{xx} = 5 \text{ mm}$, $L_1 = 1.2 \text{ mm}$, $L_2 = 1 \text{ mm}$, $X_1 = 10 \text{ mm}$, $X_2 = 8.2 \text{ mm}$, $X_3 = 9 \text{ mm}$, $Y_1 = 3.68 \text{ mm}$, $Y_2 = 5 \text{ mm}$, $Y_3 = 3 \text{ mm}$, and $Y_4 = 7 \text{ mm}$.

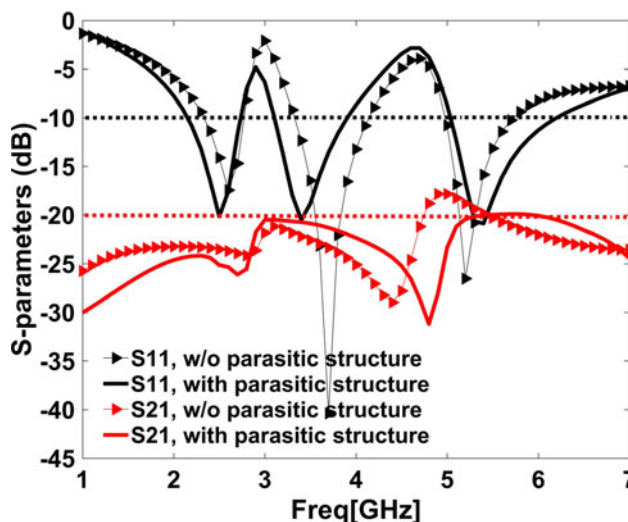


Fig. 9. MIMO antennas S_{11} and S_{21} with and without T-bar parasitic element.

MIMO antenna performance analysis

To scrutinize the role of L-shaped elements on the MIMO antenna performance, Fig. 5 shows the MIMO antenna design process step by step. As can be seen, in each step, some part of

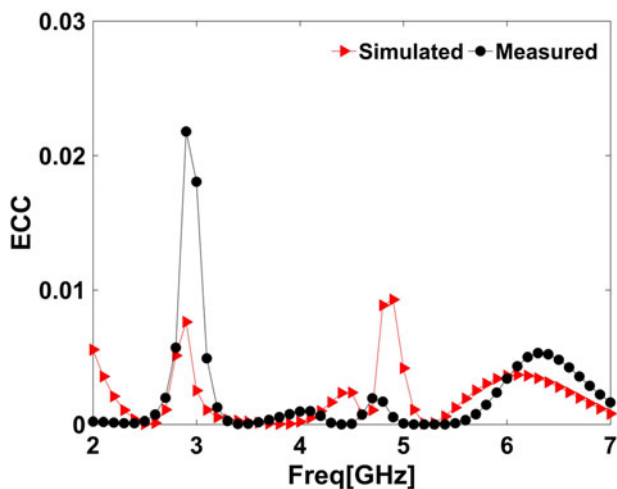


Fig. 10. Simulated and measured ECC curve for the proposed MIMO antenna.

the radiating patch branches is included in the antenna structure to reveal the role of that element in the formation of final performance. The corresponding S_{11} curves of the aforementioned four antennas are plotted in Fig. 6. As can be seen, Ant. 1, which includes one L-shaped structure and a microstrip line, covers a band of 4.8 to 6.7 GHz. By adding one other section of the radiating patch in Ant. 2, a dual band operation is observed. The obtained frequency bands are 2.4–3.1 GHz and 5–5.6 GHz. In the third step, the inclusion of all the L-shaped elements, a triple-band operation with central frequencies of 2.7, 3.2, and 5.4 GHz is observed. Finally, in Ant. 4, the T-band parasitic element is included to finalize the antenna topology. As the results indicate, the operating frequency bands are slightly shifted toward higher frequencies. The proposed MIMO antenna operates over three frequency bands. The first obtained bandwidth is 2.15–2.73 with a central frequency of 2.4. The second one is 3.1–3.9, with a central frequency of 3.4, and the third one extends from 5.04 to 6 GHz with a central frequency of 5.4 GHz. The obtained isolation level is more than 20 dB.

It is worth noting that the above mentioned obtained results are in line with the theoretical governing mathematical formulation as mentioned in (1) in previous sections. The mathematical formula in (1) indicates that as the length of the conductive element increases, the excited frequency shifts toward lower frequencies. In Ant. 1, the excited resonance is around 5.5 GHz. This is while in Ant. 2, where the length of the conductive element on the radiating patch is increased, another resonance is excited at lower frequencies at about 2.7 GHz. In Ant. 3, another L-shaped element is included which is shorter than the conductive elements in Ants. 1 and 2. As it is expected, the excited resonance is between the resonance frequencies excited by Ants. 1 and 2. Obviously, the simulated results are confirmed by the theoretical discussions.

The obtained results regarding the three band operation could be justified by surface current distribution too. Figure 7 shows the surface current distribution on the MIMO antenna at three sample frequencies selected at three operating bandwidths. As can be seen, at 2.4, 3.5, and 5.5 GHz different parts of the radiating patch radiate effectively. These are the elements which contribute at antenna performance at relevant frequency.

To scrutinize the effect of T-bar parasitic element on inter-element isolation, the MIMO antenna configuration with and

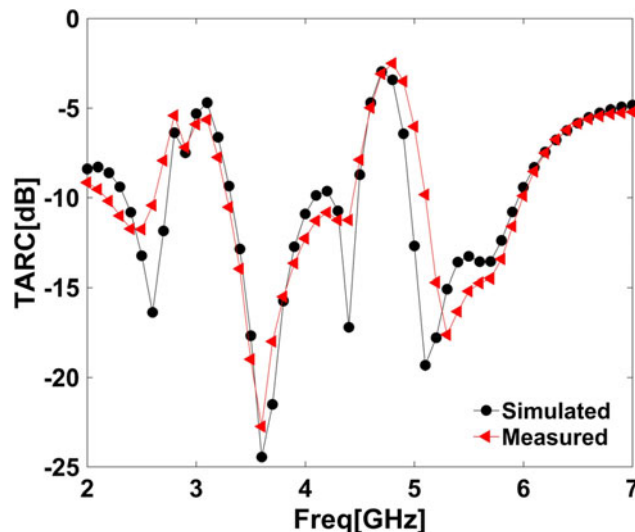


Fig. 11. Simulated and measured TARC curve for the proposed MIMO antenna.

without the parasitic element is shown in Fig. 8. Corresponding S_{11} curves are also plotted in Fig. 9. As can be seen, by the inclusion of the parasitic element, the first and second operating frequency bands are shifted toward lower frequencies. This is while the third bandwidth is widened from the higher edge. Most importantly, the S_{21} curve which corresponds to the isolation level is enhanced significantly with the embedment of the parasitic element. This observation is even more dominant over the first and third bands.

Two metrics which are used to discuss how independent the antennas work beside each other, are envelope correlation coefficient (ECC) and total active reflection coefficient (TARC). ECC shows the independency of the antennas radiation patterns. The lower values of ECC correspond to more independency of the antennas. ECC is calculated based on the following formulation:

$$ECC = \frac{|S_{11}^* S_{12} + S_{21}^* S_{22}|^2}{(1 - |S_{11}|^2 - |S_{21}|^2)(1 - |S_{22}|^2 - |S_{12}|^2)} \quad (2)$$

As mentioned, lower values of ECC show higher isolation. The simulated and measured ECC curve for the proposed MIMO antenna is plotted in Fig. 10. As can be seen, in the case of both simulation and measurement, ECC is not more than 0.03 over the entire frequency band in both simulation and measured results. This range confirms the suitable isolation of the constituent antenna elements.

Moreover, as the other parameter, TARC is defined as the square root of the ratio of total reflected power to the total incident power and its apparent return loss of the overall MIMO antenna system. In the case of MIMO antenna which comprise two antenna elements, TARC is calculated as follows:

$$TARC = \sqrt{\frac{(S_{11} + S_{12})^2 + (S_{21} + S_{22})^2}{2}} \quad (3)$$

TARC values lower than 0 dB are desired in MIMO systems. Simulated and measured TARC values are depicted in Fig. 11. It is clearly seen that suitable results are obtained in both simulation and measurement.

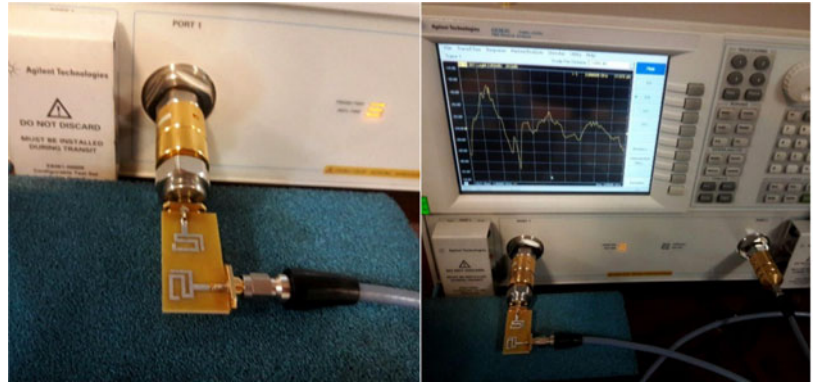


Fig. 12. Fabricated MIMO antenna under measurement process.

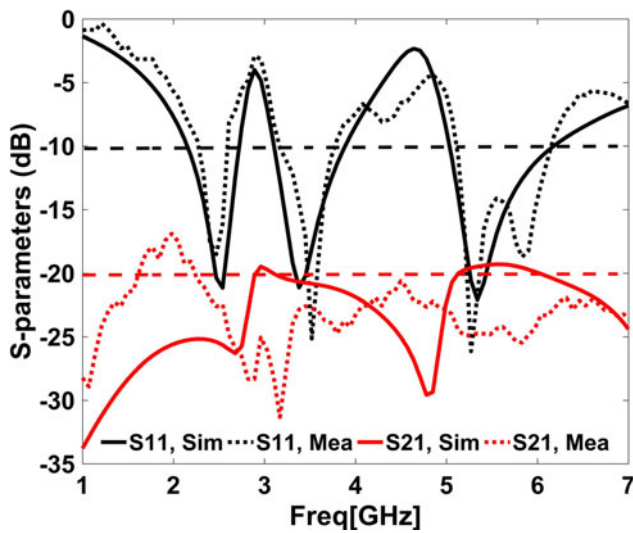


Fig. 13. Simulated and measured S_{11} and S_{21} for the proposed MIMO antenna.

Results and discussion

To assess the validity of the obtained simulated results, a prototype is fabricated and measured in antenna and microwave laboratory. The fabricated prototype which is connected to PNA (EVA368) E8363C for S-parameters measurement is shown in Fig. 12. The simulated and measured S_{11} and S_{21} performance are shown in Fig. 13. The results indicate that the antenna has a bandwidth (for $S_{11} < -10$ dB) of 2.15–2.73 with a central frequency of 2.4, 3.1–3.9 with a central frequency of 3.5, and 5.04–6 GHz with a central frequency of 5.5 GHz. Moreover, the isolation (in terms of S_{21}) is below 20 dB at the same frequency band. Simulated and measured results confirm each other.

Apart from the S parameters, peak gain and radiation efficiency of the proposed MIMO antenna is also studied in Fig. 14. An efficiency of about 90% with gain values between 2 and 4 dBi is observed for the antenna. As mentioned earlier, group delay of the antenna is an important parameter which should be considered in antenna performance analysis. Figure 15 shows the antenna group delay. It is seen that less than 1.5 ns variation is obtained for the antenna. Antenna radiation patterns at six different frequencies are plotted in Fig. 16. The results confirm the suitability of the radiation patterns in xz and yz planes.

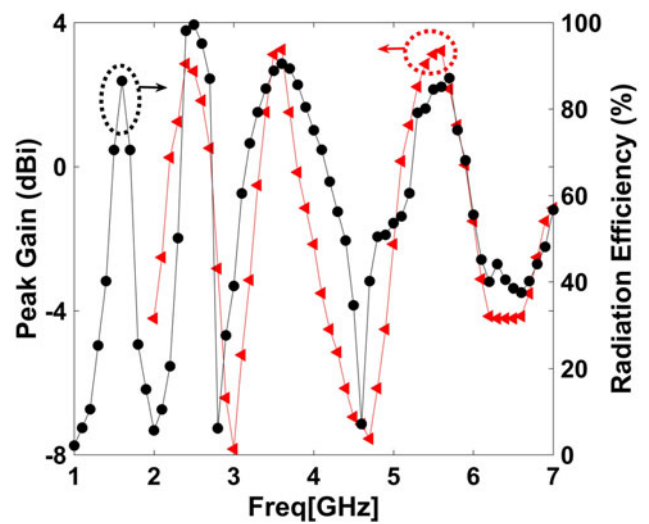


Fig. 14. Simulated peak gain and radiation efficiency for the proposed MIMO antenna.

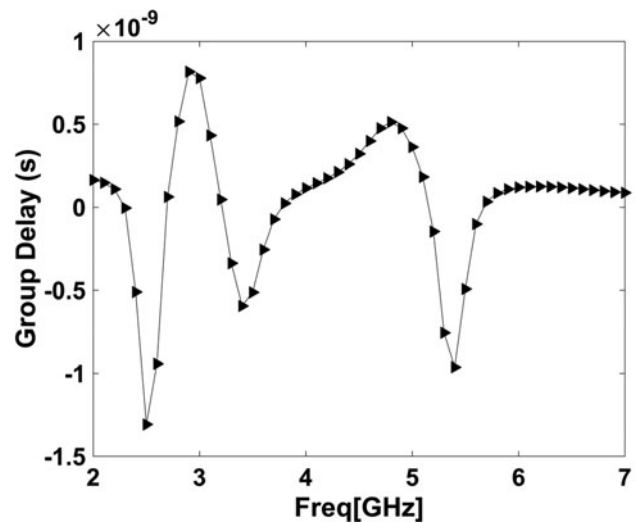


Fig. 15. Simulated group delay for the proposed MIMO antenna.

Comparison

To clarify the advantages of proposed design over previously designed similar structures, a comprehensive comparison is carried out. The comparison terms include antenna dimensions, operating

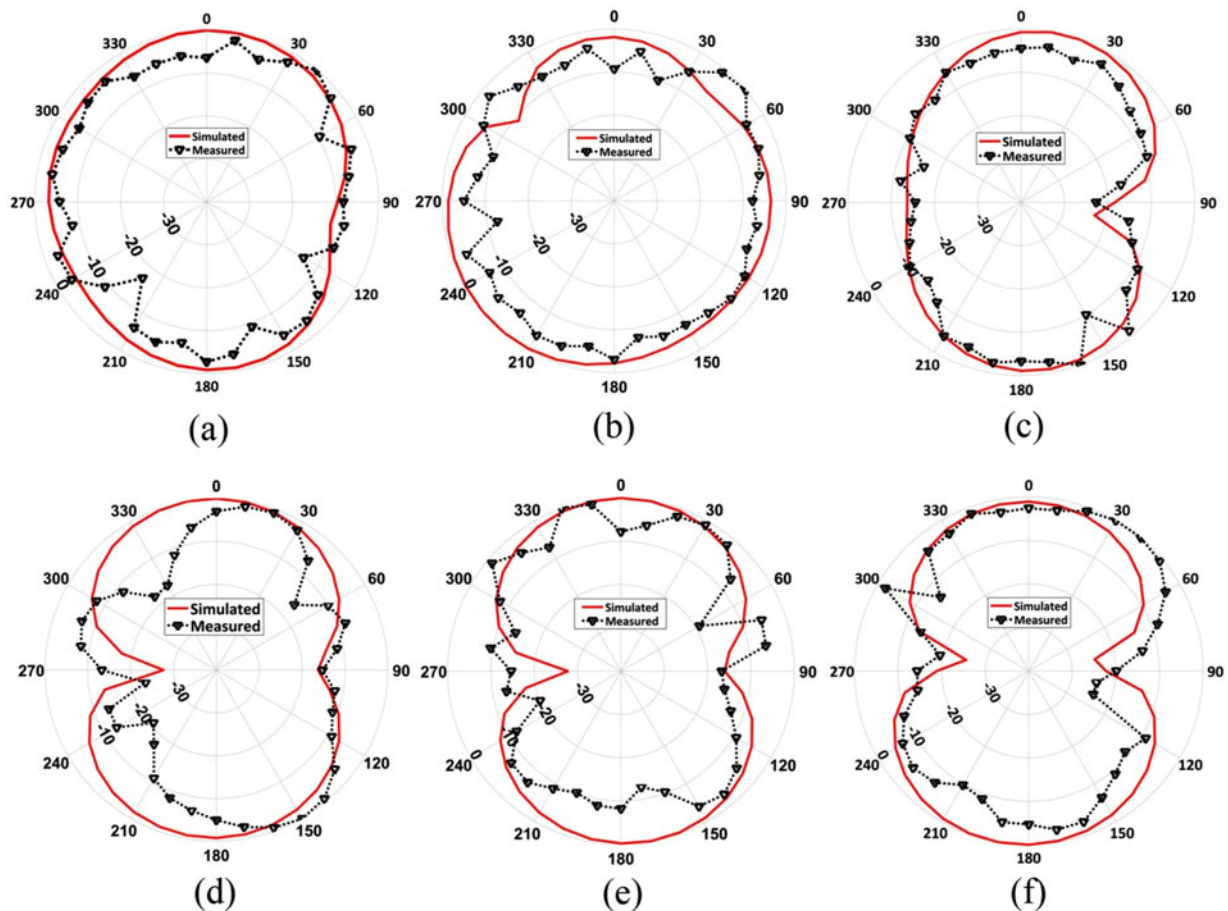


Fig. 16. The radiation pattern of the proposed MIMO antenna in (a) 2.4 GHz, (b) 3.5 GHz, (c) 5.5 GHz in the Y-Z plane and (d) 2.4 GHz, (e) 3.5 GHz, and (f) 5.5 GHz in the X-Z plane.

frequency bands, and isolation between antennas. Table 1 summarizes the results. The provided data show that the proposed antenna has a compact size. The antennas in [18–23] although having larger sizes which yield more freedom degree but provide less or equal frequency bands as the antenna in this paper. Moreover, the isolation status is better than the antennas in [18–23]. A brief comparison reveals the superior performance of the antenna in this work.

Conclusion

In this article, a very compact structure (20×40 mm) is designed and built for portable multifunctional applications. The design is very simple and cost-effective, and the proposed MIMO antenna consists of two antennas with four L-shaped structures in each of the radiation elements and a ground plane for each monopole antenna. Using these L-shaped structures, the MIMO antenna covers the bands 2.15–2.73 with a central frequency of 2.4, 3.1–3.9 with a central frequency of 3.5, and 5.04–6 GHz with a central frequency of 5.5 GHz. In order to increase the isolation between the elements, a T-shaped parasitic structure was placed between the monopole elements to reduce the isolation to below 20 dB. Small size, simple structure, and high isolation are some of the benefits of this designing. In addition, the simulated results and the measurements of are confirmed each other. Eventually, the proposed MIMO antenna can be introduced as a convenient antenna for portable wireless and multi-band applications.

References

1. Wu L and Xia Y (2017) Compact UWB-MIMO antenna with quad-band-notched characteristic. *International Journal of Microwave and Wireless Technologies* 9, 1147–1153.
2. Wu L, Xia Y, Cao X and Xu Z (2018) A miniaturized UWB-MIMO antenna with quadruple band-notched characteristics. *International Journal of Microwave and Wireless Technologies* 10, 948–955.
3. Manohar M, Kshetrimayum RS and Gogoi AK (2019) Low profile dual band-stop super wideband printed monopole antenna with polarization diversity. *International Journal of Microwave and Wireless Technologies* 11, 1–9.
4. El Bakouchi RJ, Brunet M, Razban T and Ghammaz A (2016) Broadband MIMO antenna for HiperLAN/2, WLAN, and WiMAX applications with high isolation. *International Journal of Microwave and Wireless Technologies* 8, 309–317.
5. Deng JY, Li JY, Zhao L and Guo L (2017) A dual-band inverted-F MIMO antenna with enhanced isolation for WLAN applications. *IEEE Antennas and Wireless Propagation Letters* 16, 2270–2273.
6. Khan A, Jamaluddin M, Aqeel S, Nasir J, Kazim J and Owais O (2017) Dual-band MIMO dielectric resonator antenna for WiMAX/WLAN applications. *IET Microwaves, Antennas & Propagation* 11, 113–120.
7. Mathialagan S (2017) Design of CPW-fed tapered MIMO antenna for ISM band applications. *International Journal of Microwave and Wireless Technologies* 9, 227–230.
8. Moradikordalivand A, Leow CY, Rahman TA, Ebrahimi S and Chua TH (2016) Wideband MIMO antenna system with dual polarization for WiFi and LTE applications. *International Journal of Microwave and Wireless Technologies* 8, 643–650.

9. **Yang Y, Chu Q and Mao C** (2016) Multiband MIMO antenna for GSM, DCS and LTE indoor applications. *IEEE Antennas and Wireless Propagation Letters* **15**, 1573–1576.
10. **Zhang Y and Wang P** (2016) Single ring two-port MIMO antenna for LTE applications. *Electronics Letters* **50**, 998–1000.
11. **Cheng C, Chen W, Lin G and Chen H** (2017) Four antennas on smart watch for GPS/UMTS/WLAN MIMO application. *International Conference on Computational Electromagnetics (ICCEM)*, pp. 346–348.
12. **XU Z, Zhang Q and Guo L** (2019) A printed multiband MIMO antenna with decoupling element. *International Journal of Microwave and Wireless Technologies* **11**, 413–419.
13. **Dai XW, Li L, Wang ZY and Liang CH** (2015) High isolation and compact MIMO antenna system with defected shorting wall. *International Journal of Microwave and Wireless Technologies* **7**, 167–172.
14. **Ding K, Gao C, Qu D and Yin Q** (2017) Compact broadband MIMO antenna with parasitic strip. *IEEE Antennas and Wireless Propagation Letters* **16**, 2349–2353.
15. **Li Z, Du Z, Takahashi M, Saito K and Ito K** (2012) Reducing mutual coupling of MIMO antennas with parasitic elements for mobile terminals. *IEEE Transactions on Antennas and Propagation* **60**, 473–481.
16. **Ansoft High Frequency Structure Simulation (HFSS), ver. 15.**
17. **Deshmukh AA and Ray KP** (2012) Formulation of resonance frequencies for dual-band slotted rectangular microstrip antennas. *IEEE Transactions on Antennas and Propagation* **54**, 78–97.
18. **Sharawi M, Ikram M and Shamim A** (2017) A two concentric slot loop based connected array MIMO antenna system for 4G/5G terminals. *IEEE Transactions on Antennas and Propagation* **65**, 6679–6686.
19. **Bai J, Zhi R, Wu W, Shangguan M, Wei B and Liu G** (2018) A novel multiband MIMO antenna for TD-LTE and WLAN applications. *Progress In Electromagnetics Research Letters* **74**, 131–136.
20. **Huang H and Xiao S** (2016) Compact MIMO antenna for bluetooth, WiMAX, WLAN, and UWB applications. *Microwave and Optical Technology Letters* **58**, 783–787.
21. **Dong J, Yu X and Deng L** (2017) A decoupled multiband dual-antenna system for WWAN/LTE smartphone applications. *IEEE Antennas and Wireless Propagation Letters* **16**, 1528–1532.
22. **Pouyanfar N, Ghobadi C, NOurinia J, Pedram K and Majidzadeh M** (2018) A compact multi-band MIMO antenna with high isolation for C and X bands using defected ground structure. *Radioengineering* **27**, 686–693.
23. **Ekrani H and Jam S** (2018) A compact triple-band dual-element MIMO antenna with high port-to-port isolation for wireless applications. *International Journal of Electronics and Communications* **96**, 219–227.



T. Azarinasab was born in 1986 in Iran. He received the B.Sc. degree in Electrical Engineering from Amol Institute of Higher Education, Amol, Iran. He is currently working toward the M.Sc degree in RF and microwave engineering at Aeen Kamal University, Urmia, Iran.



Ch. Ghobadi was born in June, 1960 in Iran. He received his B.Sc. in Electrical Engineering Electronics and M.Sc. degrees in Electrical Engineering Telecommunication from Isfahan University of Technology, Isfahan, Iran and Ph.D. degree in Electrical-Telecommunication from University of Bath, Bath, UK in 1998. From 1998 he was an Assistant Professor and now he is a Professor in the Department of Electrical Engineering of Urmia University, Urmia, Iran. His primary research interests are in antenna design, radar, and adoptive filters.



Burhan Azarm was born in 1992 in Iran. He received the B.Sc. degree in Power Engineering from Islamic Azad University and M.Sc. degrees in Electrical Engineering Telecommunication from Urmia University. He is currently working toward the Ph.D. degree in RF and microwave engineering at Urmia University. His research interests include Antennas, Microwave, and Electromagnetics.



M. Majidzadeh was born in 1987 in Urmia, Iran. She received her Ph.D., M.Sc. and B.S. degrees in Electrical Engineering from Urmia University in 2016, 2012, and 2009, respectively. Now she is an assistant professor in Department of Electrical and Computer Engineering, Urmia Girls Faculty, West Azarbaijan branch, Technical and Vocational University (TVU), Urmia, Iran. Her research interests are in electromagnetic compatibility, frequency selective surfaces, MIMO antennas, antenna bandwidth enhancement and antenna miniaturization techniques, circularly polarized antennas, and numerical method in electromagnetics.